

Article

Development of Oxygen-Plasma-Surface-Treated UHMWPE Fabric Coated with a Mixture of SiC/Polyurethane for Protection against Puncture and Needle Threats

Dariush Firouzi ¹, Chan Y. Ching ¹, Syed N. Rizvi ² and P. Ravi Selvaganapathy ^{1,*} 

¹ Department of Mechanical Engineering, McMaster University, Hamilton, ON L8S 4L7, Canada; dariush.firouzi@gmail.com (D.F.); chingcy@mcmaster.ca (C.Y.C.)

² RONCO, 70 Planchet Road, Concord, ON L4K 2C7, Canada; rizvi.n.syed@gmail.com

* Correspondence: selvaga@mcmaster.ca; Tel.: +1-(905)-525-9140 (ext. 27435)

Received: 28 March 2019; Accepted: 13 May 2019; Published: 20 May 2019



Abstract: Although considerable research has been directed at developing materials for ballistic protection, considerably less has been conducted to address non-firearm threats. Even fewer studies have examined the incorporation of particle-laden elastomers with textiles for spike, knife, and needle protection. We report on a new composite consisting of ultra-high-molecular-weight polyethylene (UHMWPE) fabric impregnated with nanoparticle-loaded elastomer, specifically designed for spike- and needle-resistant garments. Failure analysis and parametric studies of particle-loading and layer-count were conducted using a mixture of SiC and polyurethane at 0, 30, and 50 wt.%. The maximum penetration resistance force of a single-layer of uncoated fabric increased up to 218–229% due to nanoparticle loading. Multiple-layer stacks of coated fabric show up to 57% and 346% improvement in spike puncture and hypodermic needle resistance, respectively, and yet were more flexible and 21–55% thinner than a multiple-layer stack of neat fabric (of comparable areal density). We show that oxygen-plasma-treatment of UHMWPE is critical to enable effective coating.

Keywords: coating; UHMWPE; nanoparticle-laden elastomer; oxygen-plasma treatment; penetration resistance

1. Introduction

In many countries around the world, non-firearm weapons have been associated with the dominant fraction of violent crimes. For instance, in Canada, about 19% of all violent crimes committed in 2016 involved the use of non-firearm weapons while only 3% were attributed to the use of firearms [1]. Due to the increasing number of assaults committed using knives and sharpened instruments, puncture and stab resistance has become increasingly important as a safety feature for body armor [2]. Resistant materials capable of providing protection against sharp objects are also of interest in a number of different occupations, such as waste processing. There is an ever-present threat of stab and knife attacks for law enforcement and military personnel [3], as well as incidences of accidental injuries due to sharp debris, broken glass, or razor wire [4] to health care and waste management workers. The main parameters which affect the penetration resistance of textiles are the areal density of fabrics, yarn linear density and mechanical properties of fibers, number of filaments per yarn, fabric weave architecture, and the number of fabric plies. There are other parameters that could affect the resistance of a multilayer textile structure against various types of threats or penetrators, such as the boundary condition of the fabric, geometry, type, mass, and the velocity of penetrator, and inter-yarn and fabric-projectile frictional force [5–8].

Typical textile-based resistant materials comprise of high-strength fibers (HSFs), such as aramid, S-glass, ultra-high molecular weight polyethylene (UHMWPE), polypyridobisimidazole (PIPD), and polyphenylene benzobisoxazole (PBO). HSFs generally possess high tensile and compressive strength, high energy absorption, and low density [9,10]. UHMWPE fibers and fabrics are used widely in the protection industry for military body armors, helmets, and personal protective equipment (PPE), such as cut-resistant gloves [11,12]. Spectra® (Honeywell International Inc., Morristown, NJ, USA) and Dyneema® (Royal DSM) are the two main commercially produced UHMWPE fibers that have the lowest density of all HSFs currently being used for armor applications [9]. Additionally, UHMWPE possesses excellent chemical resistance and also high resistance against physical degradation [13], which makes this material a promising substitute for Kevlar® (DuPont) for body protection. Despite the many advantages of using UHMWPE fibers and fabrics for armor applications, there are considerably fewer research studies of this polymer as compared to Kevlar® (DuPont) for body armor application. Here, we exclusively summarize previous research works related to the use of UHMWPE fabric for improved penetration resistance against non-ballistic threats (such as stab, puncture, and needle penetration) and discuss related mechanisms.

Coating fabric with polymeric materials without particle addition is one simple method to improve its penetration resistance. For example, puncture resistant UHMWPE fabrics have been developed using Nylon 6,6 and Nylon 6,12 coatings. The normalized spike puncture resistance of a multiple-layer stack of UHMWPE fabric was improved up to 62% from nylon coating due to the mechanical-interlocking mechanism of the nylon solution upon washing and drying [2,14].

The impregnation of textiles with shear thickening fluids (STFs) is a relatively new approach to improve the penetration resistance of HSFs [15–22]. Interestingly, most of these studies use Kevlar® fabric and only a few have focused on the use of considerably lower-cost and lighter UHMWPE fabrics. In one particular study, it was shown that the effectiveness of STF-impregnation in improving the penetration resistance of UHMWPE fabric is dependent on fabric structure. For instance, STF-impregnation was a detrimental treatment for penetration resistance (against a spherical-head impactor at 4.5 m/s) of 400-denier UHMWPE fabrics (various thread counts except 25 × 25). On the contrary, STF-impregnation of 1350-denier UHMWPE provides up to 59% higher normalized penetration resistance force [15]. The effectiveness of STF-impregnation on UHMWPE fabric against spike and knife penetration also depends on the choice of dispersing medium used in the fabrication of STF. For instance, UHMWPE fabric impregnated with polyethylene glycol (PEG400)-based STF material even has a slightly lower stab resistance force to spike threat compared to neat fabrics [16]. Apart from the varying performances reported, one potential limitation of STF-treatment technology is the propensity of fluid-like STF materials to leakage [17], as they could be easily washed away when exposed to water and moisture [18]. In general, the mechanism of improvement of penetration resistance of STF-treated textiles is a combination of impact energy absorption due to shear thickening phenomenon and also increased inter-yarn friction [15,19].

More recently, a different technology using particle-laden elastomeric mixtures with textiles has been examined for enhanced penetration resistance. In one study, it was shown that high density polyethylene (HDPE) fabric impregnated with a mixture of heavily-loaded silica and SiC nano-sized particles (65 wt.% and 80 wt.%) in polydimethylsiloxane (PDMS) mixture provides up to 190% increase in normalized penetration resistance force to 21G hypodermic needles when it was compared to the neat fabric. The improvement in penetration resistance of treated fabrics was related to the elastic-jamming phenomenon at a very high concentration of particles [3]. Despite their promise, such nano-particle elastomer composites are difficult to incorporate into UHMWPE fabrics and to the best of authors' knowledge, studies on spike puncture resistance of particle-elastomer impregnated UHMWPE fabrics have not been reported elsewhere.

Here, we show that oxygen plasma-treatment is an effective method for impregnating the nanoparticle elastomer material into UHMWPE fabrics. Using this method, we demonstrate for the first time new textile composites that have superior spike and needle puncture resistance and study

the influence on the composition of these composites on the resistance conferred. Various samples were developed for penetration tests using UHMWPE fabric impregnated with different mixtures of SiC particles in a polyurethane (PU)-based elastomer. Our developed formulation and coating method has a good potential to be applied to protective garments or gloves.

2. Penetration Tests and Characterization

2.1. Materials

The UHMWPE plain woven fabric (Spectra[®] 900) with an areal density of 230 g/m², 1200 denier, 1333 dtex, and thread-count of 21 × 21 yarns per inch was supplied by Barrday Inc., Charlotte, NC, USA. The silicon carbide (SiC) particles from Panadyne Inc. Montgomeryville, PA, USA, had a nominal diameter of 0.5 μm and specific surface area of 4–8 m²/g. A polyurethane-based elastomer (Brush-On[®] 40 kit, Smooth-On, Inc., Macungie, PA, USA) with 1000% elongation at break and density of 1170 kg/m³ was purchased from Smooth-On, Inc., Macungie, PA, USA. The kit was comprised of A and B components to be mixed in a 1:1 ratio by weight. An organic solvent (mineral spirit) was purchased from Recochem Inc., Milton, ON, Canada.

2.2. Fabric Preparation-Plasma Treatment

UHMWPE fabric was cut to 12 cm × 18 cm and then put in a capacitively-coupled systems plasma chamber (PE-25, Plasma Etch, Inc., Carson City, NV, USA) with a radio frequency (RF) source at 50 kHz and vacuumed at around 18×10^{-2} Torr. Oxygen was then fed into the chamber (50 cc/min) for 60 s during gas stabilization phase. The oxygen feed was then closed before the RF power was applied for 5 min with power of 300 W. The plasma treatment was found to increase the adhesion of UHMWPE to coating materials.

2.3. Coating Preparation

Organic solvent (mineral spirit) was added to the pre-polymer base part of Brush-On[®] 40 kit, so the weight ratio of solvent to part A was 3.5 and was mixed thoroughly for 2 h. SiC particles were then added to the mixture to 30 wt.% and 50 wt.% of the final mixture (i.e., the total weight of particles and parts A and B of the elastomer) and mixed for 3 h. Paste-like part B of the elastomer kit was then added to the well-dispersed mixture and stirred thoroughly for 30 min. At this point, the mixture had a low viscosity, which made an immersion (dip) coating process feasible without additional equipment. The plasma-treated fabric samples were soaked (dipped) in the mixture for 15 s and hang-dried for five hr. Using this technique, the material pickup of fabric samples from a same coating mixture is fairly equivalent, although the samples were not squeezed after the dip process. One general advantage of the dip coating technique is that fibers are not stressed or distorted during such a process [23]. Figure S1 in Supplementary Information shows a schematic of the fabrication process and plasma treatment setup.

2.4. Spike Puncture and Needle Penetration Tests

Spike puncture penetration tests were performed according to the European standard for protective gloves against mechanical risks (EN 388:2016 standard), which is also suggested by the American National Standard Institute/International Safety Equipment Association (ANSI/ISEA 105-2016 standard). Using a SHIMADZU tensile tester with 500 N load cell, a steel stylus-like spike (Figure 1b) with a diameter of 4.5 mm (nose diameter of 1 mm) was pushed through the fabric sample at a traverse speed of 100 mm/min. The supporting fixture for the fabric was made in a similar manner to the EN 388 standard, with an open internal diameter of 20 mm (Figure 1a). The fabric sample was held (sandwiched) firmly between the supporting fixture and another plate with the same open internal diameter, using four clamps at the directions of warp and weft fibers. Each test was repeated at least

ten times and the maximum resistance force was recorded. In a similar fashion, multiple-layer stacks of fabric were tested.

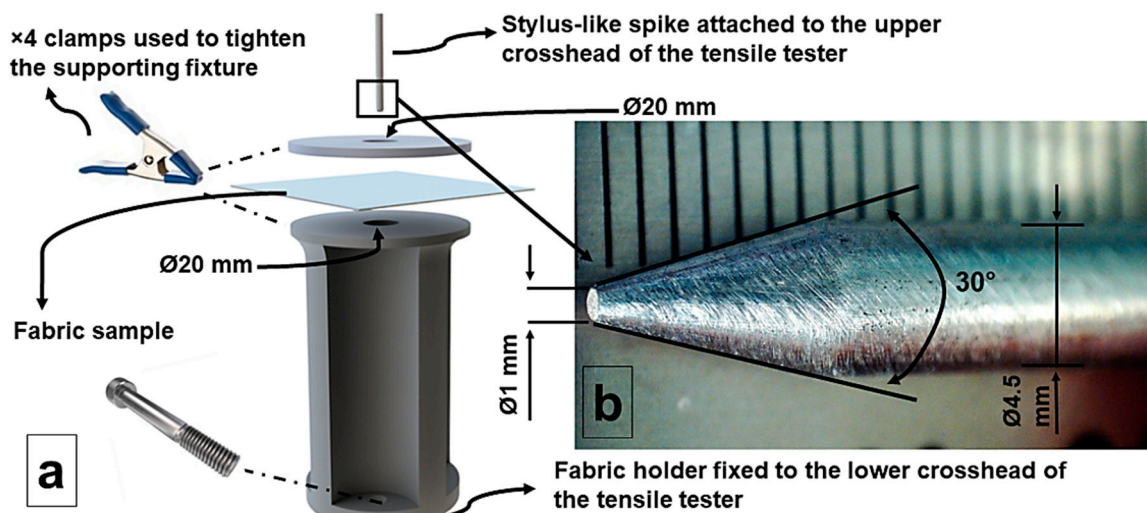


Figure 1. (a) Schematic of penetration test setup. (b) Stylus-like spike, according to EN 388:2016 standard (millimeter-scale).

Target samples were then categorized into different levels based on their maximum resistance against spike puncture (Table S1 in Supplementary Information). Hypodermic needle penetration tests were performed similarly to a previous study [3] and in accordance with the American Society for Testing and Materials (ASTM F2878–10 standards). Briefly, the fabric sample was held firmly between the supporting fixture and another plate with the same open internal diameter of 20 mm. The fabric target was then punctured by the needles at a speed of 500 mm/min. A fresh 25G 1" (BD 305125) hypodermic needle was used for each test and repeated at least ten times and the maximum resistance force was recorded. Samples were then categorized into different levels based on their maximum resistance against hypodermic needle according to ANSI/ISEA 105-2016 (Table S1 in Supplementary Information).

2.5. Flexibility Test and Coefficient of Friction Determination

Flexibility tests were performed similar to our previous work [3], based on the principles of ASTM D1388. The objective of this test was to compare the rigidity of samples before and after coating. A 5 cm × 10 cm piece of each sample was cut and encapsulated inside a thin polyethylene bag and a 20 g weight was attached to its leading edge at mid-point. With 6.2 cm length of the sample held firmly on the edge of table, its bending angle (BA) is then measured from captured images. A higher bending angle from this test means higher flexibility of the sample. Static coefficient of friction of neat fabrics (before and after plasma treatment) along the weft direction were calculated according to ASTM D1894-14, using a SHIMADZU tensile tester with 500 N load cell (Method-C of apparatus for assembly).

2.6. Image Analysis and Contact Angle Measurement

The images were taken using a handheld digital microscope (Celestron Acquisition, LLC, Torrance, CA, USA). Scanning electron microscopy (SEM) analysis was done using a VEGA-LSU TESCAN VP. Optical contact angle measurements were done using a DataPhysics OCA-35 instrument to analyze wettability of the fabric surface before and after plasma treatment. A drop of Milli-Q® (MilliporeSigma, Burlington, VT, USA) ultrapure water (dosing rate of 2 $\mu\text{L/s}$) was applied using the instrument's electronic syringe unit on the surface of the sample and the corresponding contact angle was recorded.

3. Results and Discussion

An initial spike test was conducted on as-received and coated plasma-treated UHMWPE fabric samples to show the effectiveness of the coating process. The images of the samples before and after puncture under a maximum pre-set load of 100 N are shown in Figure 2. The top row shows the spike penetration of a 3-layer stack of neat fabric and the bottom row shows the same penetration test on a 2-layer stack of oxygen-plasma-treated coated fabric (with 50 wt.% of SiC in PU mixture) of a comparable areal density. It can be seen that the 3-layer neat fabric sample was easily penetrated, and fibers were pushed aside at the impact area. This is a typical “windowing mechanism” in textiles under the impact of a spike or similar sharp pointed objects [2,3]. On the contrary, the 2-layer stack of coated fabric sample was not penetrated and only a small dent was visible on the surface.

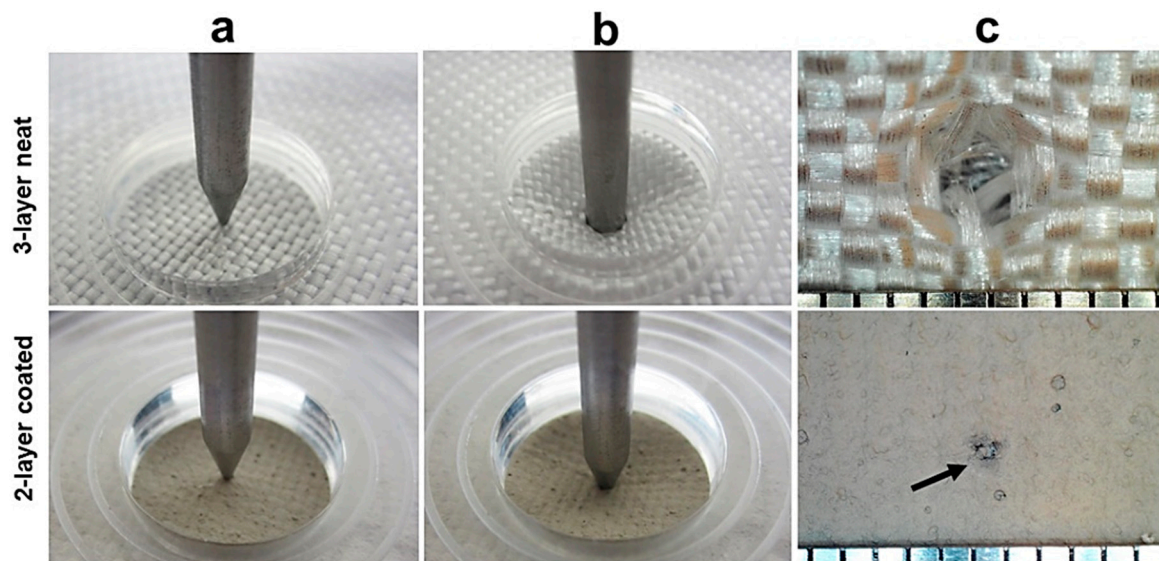


Figure 2. Images of the fabric samples undergoing the spike penetration test under a maximum pre-set load of 100 N: (a) start of penetration; (b) end of penetration; (c) top close view of the impact area. The top row is a 3-layer stack of neat fabric, while the bottom row is 2-layer stack of coated fabric with 50 wt.% SiC in polyurethane (PU). The arrow shows the point of contact on the coated sample (millimeter-scale).

In order to understand the results better, the material was microscopically analyzed. The SEM images of untreated fabric with only PU coating are shown in Figure 3a. It is seen from the figure that the coating material is not uniform and poorly bonded to the fabric substrate. Similar observations can be made for the coated fabric with 30 and 50 wt.% SiC in a PU mixture from Figure 3b,c, respectively. On the other hand, plasma-treated fabric with PU coating (Figure 3d) showed improved coating uniformity. Similar improvement in uniformity of the coating material was also observed in particle-laden PU coatings (comparing Figure 3e to Figures 3b and 3f to Figure 3c). The areal density of coated samples increased by about 2–5% when the fabrics were plasma-treated and coated, which indicates a better wettability and higher absorption of the coating material onto fibers. Since plasma treatment has been used in the past to open reactive groups on textile surfaces to functionalize them [23], this behavior is expected. UHMWPE fiber with low surface energy and a smooth surface is inherently inert and not a good host to bond with other materials [2,13]. Through plasma treatment, polarizable groups can be introduced that will enhance wettability and also bonding to other matrix materials. For instance, plasma treatment has been used to improve adhesion between UHMWPE and HDPE matrices, which resulted in higher interlaminar shear strength (ILSS), tensile strength, and impact strength of the fabricated composites [24]. Similarly, plasma treatment of UHMWPE fibers also improves interfacial bonding with epoxy resin, resulting in higher tensile strength but considerably lower

elongation [13]. In general, oxidative RF-plasma treatment could effectively improve wettability and surface characteristics of polyethylene by creating oxygen-based functionalities [25]. More specifically, the surface modification of UHMWPE through oxygen plasma-treatment is likely due to the formation of carbon–oxygen functional groups (such as C–O, C=O, O=C–O) and cross-linking of UHMWPE molecules, which contribute to the increased surface free energy and hydrophilic transformation of the oxygen-plasma-treated polymer [26,27]. The water contact angle of the as-received UHMWPE fabric was $120.7 \pm 3.6^\circ$, which can be considered as a hydrophobic material. However, when a droplet of water was dropped on the surface of the UHMWPE fabric, which was treated with plasma for 1/6min, 1/2min, 1min, 2min, 3min, 4min, and 5 min, the water instantly spread over the surface of the fabric, indicating complete wetting of the plasma-treated fabric. The change of contact angle confirms the remarkable change in surface properties from an inert material to one that has polarizable groups and open dangling bonds, which could be beneficial for wettability and adhesion of coatings to the UHMWPE fabric (Figure 3a–f).

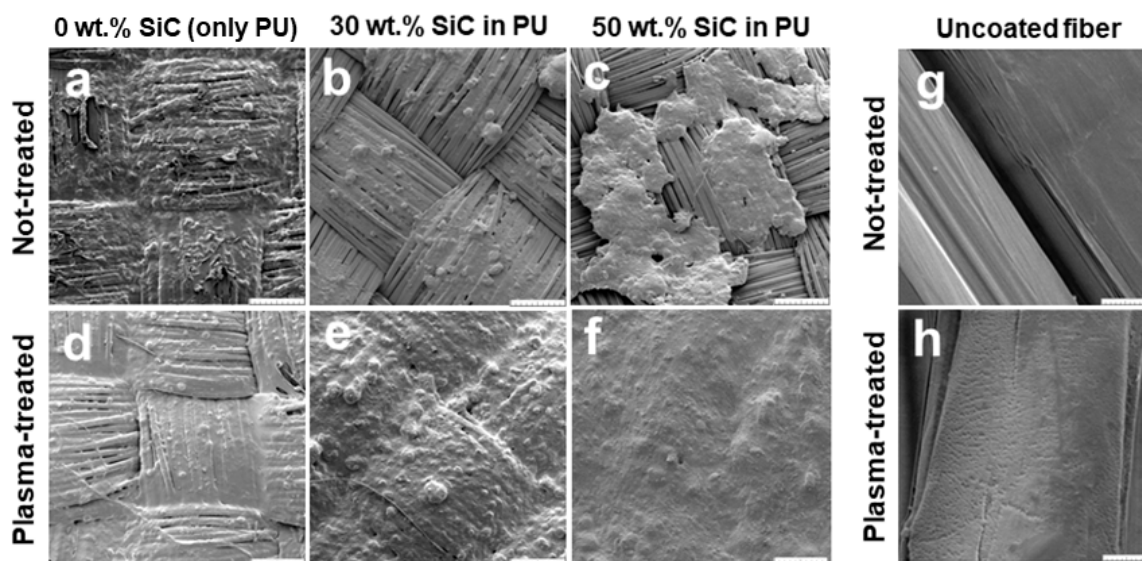


Figure 3. (a–f) Top view before-puncture test scanning electron microscope (SEM) images of plasma-treated and not-treated ultra-high molecular weight polyethylene (UHMWPE) fabrics coated with different mixtures of SiC in PU. The scale bar is 500 μm . (g,h) Plasma-treated and not-treated UHMWPE fibers. The scale bar is 10 μm .

The SEM images of UHMWPE fibers after plasma treatment (Figure 3h) reveal the presence of micro-pits onto the surface, while the as-received fiber appears perfectly smooth (Figure 3g). The presence of such micro-pits onto the surface of plasma-treated fibers could improve adhesion of UHMWPE fibers through a mechanical interlocking mechanism [28]. This observation is in agreement with the results for the coefficient of friction. The static coefficient of friction of UHMWPE fabric increased from 0.20 ± 0.08 to 0.38 ± 0.12 when it was plasma-treated for 5 min due to its higher roughness, which was due to the presence of micro-pits.

3.1. Puncture Test Results

A single-layer neat plasma-treated UHMWPE fabric and single-layer samples of plasma-treated UHMWPE fabric coated with 0 wt.%, 30 wt.%, or 50 wt.% concentrations of SiC were tested to study the influence of the particle loading on puncture resistance against a spike threat. The typical force-displacement curves of 1-layer plasma-treated neat and coated plasma-treated fabrics against spike penetration are shown in Figure 4a. The resistance force increases when the tip of the penetrator comes in contact with each of the samples. A first load peak occurs at about 3–6 mm of penetration

distance in all three coated samples, which matches the length of the conical tip of the spike shown in Figure 1b. At the first peak, an audible burst sound was heard, which is correlated to the breakage of adjacent fibers as the tip of the spike pierced through the samples [2]. The average resistance force of the coated plasma-treated fabric at the first peak load is 28.3 ± 4.3 N, 55.3 ± 8.2 N, and 67.3 ± 6.8 N when the concentration of SiC is 0wt.%, 30wt.%, and 50 wt.%, respectively. This means that the resistance force of primary fibers in contact with the spike at the impact area increases when more SiC is added to the mixture of PU coating.

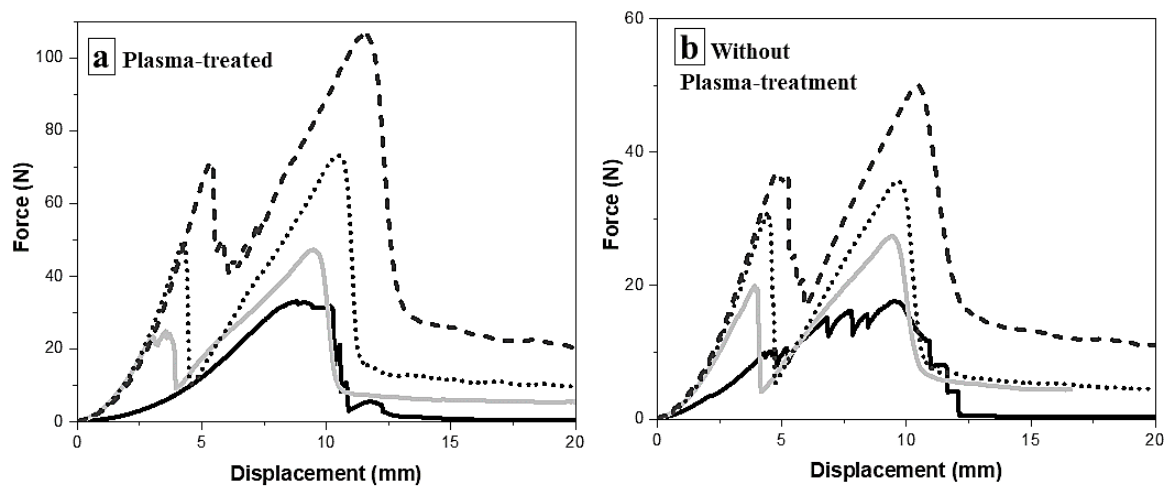


Figure 4. Force-versus-displacement curves from the spike penetration test on single-layer UHMWPE fabric samples: —, neat; — (gray color), coated with PU; •••, coated with 30 wt.% SiC in PU; —, coated with 50 wt.% SiC in PU.

After the first peak, there is a sudden drop in the force in all three coated samples followed by an increase till the force reaches a second peak. The first peak and the sudden drop can be correlated to the point when the conical tip of the spike completely passed through the sample. The increase in the penetration force after the first peak can be attributed to the resistance from distant fibers near the impact zone. The average resistance force at the second peak-load (maximum resistance force) is 45.7 ± 4.5 N, 67.3 ± 8.3 N, and 105.7 ± 9.3 N when the concentration of SiC was 0 wt.%, 30 wt.%, and 50 wt.%, respectively.

The load drops after the second peak as the conical tip of the spike completely penetrates through the fabric and adjacent fibers provide minimal further resistance. The plasma-treated neat fabric shows only a single peak of 33.2 ± 8.7 N. In this case, unlike the coated fabric samples, the distant fibers do not exert a force to the spike penetrator when the failed fibers are pushed aside. This behavior can be attributed to the lower fiber-to-fiber and fiber-to-impactor frictional forces when the UHMWPE fabric is not coated.

Additionally, Figure 4b shows the force-displacement curves from spike penetration tests of neat and coated fabric samples without prior oxygen-plasma treatment. Comparing these results with those in Figure 4a, plasma treatment increases the spike penetration resistance force of one-layer coated and uncoated fabric samples. The penetration resistance force of one-layer neat and coated fabric with 0 wt.%, 30 wt.%, and 50 wt.% SiC in PU decreased by about 35%, 47, 51%, and 54%, respectively, when the fabric was not plasma-treated.

Visual images of both the top and rear of the penetrated fabric (with or without prior plasma treatment) were taken and are shown in Figure 5 along with SEM images. In the case of the fabric coated with only the elastomer (only PU), the top view did not show any meaningful difference as compared to the rear view (Figure 5a,d), and therefore it was chosen to be represented. From the visual images (Figure 5a–f), it was observed that all the three plasma-treated samples show a good coverage of the nanoparticle/elastomer material. On the contrary, the coating material is not uniform when the

fabric is not plasma-treated prior to the coating process. A closer view of the damage zone is shown in Figure 5g–l. It can be clearly seen from Figure 5g that the PU coating forms a shell on top of the untreated fabric, while in Figure 5j the PU is well integrated with the fibers of the fabric. A similar contrast is also observed between the untreated (Figure 5h,i) and the treated (Figure 5k,l) fabrics as the particle loading in the elastomer mixture is increased to 30% and then 50%. These results demonstrate that the plasma treatment plays a critical role in the penetration of the nanoparticle-loaded PU onto the individual filaments, as opposed to the untreated case, where it forms a thin shell with poor bonding to the fibers. The integration of the nanoparticles into the depth of the fabric and between filaments is crucial in providing higher resistance to puncture. Furthermore, the coating material was found to be increasingly more damaged and peeled-off when the loading of nanoparticles was increased from 0 wt.% to 50 wt.% of the PU mixture onto fabric without prior plasma treatment. From Figure 5j–l, the effectiveness of plasma-treatment to improve adhesion and bonding strength of coating material to UHMWPE fabric is significant at all the loading concentrations of SiC nanoparticles in PU mixture. Overall, the extent of the damage is lesser for the plasma-treated fabric rather than the untreated one.

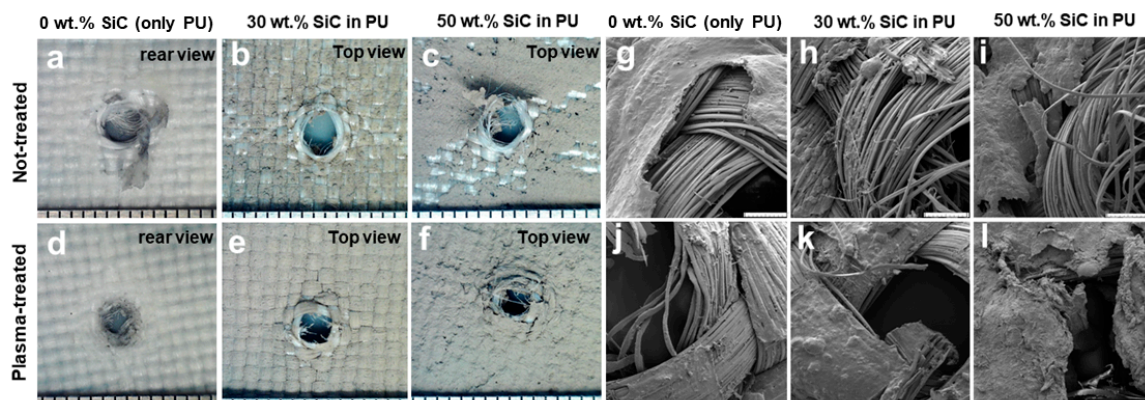


Figure 5. (a–f) Top and rear views of plasma-treated and not-treated UHMWPE fabrics coated with different mixtures of SiC in PU after penetration. (g–l) SEM images (top view) of plasma-treated and not-treated UHMWPE fabrics coated with different mixtures of SiC in PU. The scale bar is 500 μm .

In one study, Kevlar 129[®] and UHMWPE fabric were coated with natural rubber (NR) and tested against a cylindrical shape penetrator with a hemispherical head at 6 m/s. It was reported that the absorbed impact energy absorption of a single-layer rubber-coated fabric was even lower than that of a neat fabric due to a lower yarn-to-penetrator frictional force [29]. On the contrary, here we showed the improvement in maximum penetration resistance of a single-layer UHMWPE fabric at a high concentration of SiC nanoparticles. One explanation is that the fibers are more coupled and yarn-to-penetrator frictional force increases with an increase in the concentration of hard nano-sized SiC particles, and thus more force is exerted to penetrate coated fabrics. In addition, the hard nanoparticles that could be loosened during penetration could also increase frictional force in a manner similar to the three-body abrasion, enhancing the overall resistance.

Puncture Test Results of Multiple-Layer Stack of Fabric Samples

Multiple layers of neat and coated fabric samples were tested to investigate the effectiveness of the coating material based on areal density, flexibility, and thickness. For this purpose, several layers of fabric samples were stacked together and tested against spike penetration. The histogram of maximum resistance force, areal density, and flexibility of plasma-treated neat and coated UHMWPE fabric samples of different stacked layers is presented in Figure 6. Among all stacks of neat fabric, only the 7-layer stack of neat fabric could provide Level5 protection. The 7-layer stack of neat fabric has comparable areal density with the following stacked samples: (i) 5-layer coated fabric with PU; (ii) 5-layer coated fabric with 30 wt.% SiC in PU; and (iii) 2-layer coated fabric with 50 wt.% SiC in PU.

The maximum resistance force of these stacked samples was found to be about 20%, 57%, and 15% more, respectively, as compared with the resistance of a 7-layer neat fabric. Interestingly, the 5-layer coated fabric with 30 wt.% of SiC in PU showed about 36% higher penetration force compared with the 2-layer coated fabric with 50 wt.% SiC in PU (of comparable areal density), although one layer of the coated fabric with 50 wt.% SiC showed the highest maximum penetration resistance among all the samples. This result indicates that the number of stacked layers also play a major role in increasing the penetration resistance of target samples, in addition to the loading of particles in the PU mixture.

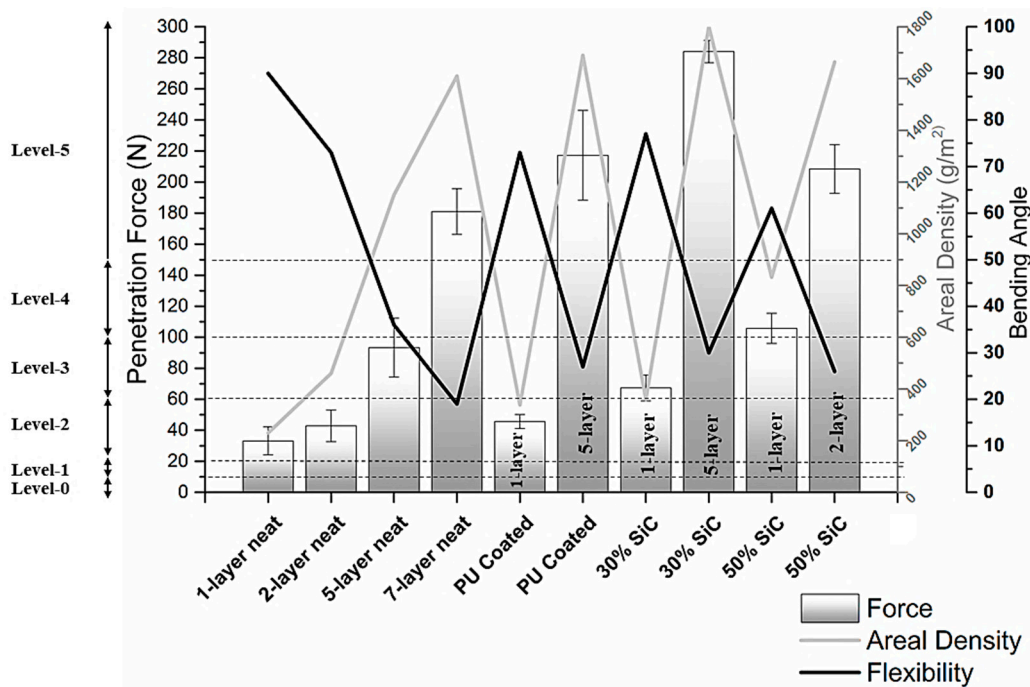


Figure 6. Measured peak resistance force, bending angle, and areal density of plasma-treated neat and coated UHMWPE fabrics of various layers undergoing spike penetration tests.

Also, from Table 1, the average thickness of a 7-layer stack of neat fabric reduced by about 21–55% compared to 2-layers and 5-layers of coated samples of comparable areal density. From Table 1, 1-layer neat fabric has the lowest rigidity, while 1-layer coated fabric with 50 wt.% SiC has the highest. Comparing the flexibility of multi-layer stacks of fabric samples with comparable areal density, it was found that the 7-layer stack of neat fabric was less flexible than 5-layer stack of coated samples with 0 wt.% and 30 wt.% of SiC, and even the 2-layer stack of coated fabric with 50 wt.% SiC in PU mixture.

Table 1. Areal density, thickness, and bending angle of plasma-treated neat and coated UHMWPE fabric samples.

No. of Stacked Fabric Layers	Particle Loading in PU Mixture (wt.%)	Areal Density (g/m ²)	Thickness (mm)	Bending Angle (θ ± 2°)
1	Neat (no coating)	230 ± 11	0.5	90
	0 (only PU)	338 ± 16	0.51 ± 0.01	73
	30	360 ± 22	0.55 ± 0.01	77
	50	832 ± 59	0.78 ± 0.09	61
7	Neat (no coating)	~1610	3.5	19
5	0 (only PU)	~1690	~2.55	27
	30	~1800	~2.75	30
2	50	~1664	~1.56	26

Apart from areal density, flexibility and thinness are equally important factors in the manufacture of protective gloves [30]. Therefore, a new figure of merit was formulated that represents the ratio of percentage increase in penetration resistance to percentage increase in thickness of different multi-layer neat and coated samples over a single layer of neat fabric and can be used to evaluate the performance of the various compositions and combinations that were fabricated. This figure of merit was found to be 0.74, 1.35, 1.68, and 2.49, respectively, for 7-layer neat, 5-layer coated with PU, 5-layer coated with 30 wt.% SiC, and 2-layer coated with 50 wt.% SiC fabrics. These results show that addition of SiC nanoparticles increases the penetration resistance significantly more as compared with any increases in thickness of the overall coated fabric. Hence, the coated sample with 50 wt.% SiC provides the optimal performance among all the samples, which is Level-5 resistance, acceptable thickness, and flexibility, without the consideration of increase in areal density.

Next, normalized penetration force of each sample was calculated based on its areal density (Table S2 in Supplementary Information). From the results, the normalized force of only 1-layer coated fabric with 50 wt.% particles is higher than 1-layer neat fabric (about 30% improvement). Furthermore, 5-layer coated fabric with 0 wt.% and 30 wt.% particles and 2-layer coated fabric with 50 wt.% particles were found to have about 14%, 40%, and 11% (respectively) higher normalized resistance force compared with a 7-layer neat fabric. In contrast, Kevlar-wool and Kevlar-wool-nylon fabrics had a surprising notable decrease in normalized penetration resistance ($N/(g/m^2)$) against a pointed impactor when they were coated with 20 wt.% silica particles (of 242 μm diameter) and a PVC binder [31]. This may be due to the higher concentration (30 wt.% and 50 wt.%) of particles used in our study to fabricate particle-laden elastomeric mixtures. The 0.5 μm SiC particles used here could also provide a better mixing homogeneity in elastomeric mixture compared with a mixture of 242 μm SiO₂ particles. Additionally, our nanocomposite also outperforms another study [32], where STF materials were impregnated into UHMWPE fabric to improve penetration resistance. There, it was reported that an 8-layer stack of STF-treated UHMWPE fabric provides approximately 21% higher normalized penetration resistance force (against a spike) compared to an 8-layer stack of neat UHMWPE fabric, and yet was about 30% thicker than the neat one [32]. Similarly, STF-treated UHMWPE composite panels have been compared with untreated UHMWPE composite panels under a drop tower impact test (using a spike-like impactor). From the results, the maximum resistance force of STF-treated UHMWPE composite panels was even lower than untreated panels and penetration resistance was not improved after STF treatment [20].

3.2. Hypodermic Needlestick Penetration

Single and multiple layers of neat and coated fabric samples of plasma-treated fabric were tested to study the impact of coating (0 wt.%, 30 wt.%, and 50 wt.% concentration of SiC) on penetration resistance against a needle threat. The typical force-displacement curves of 1-layer plasma-treated neat and coated plasma-treated fabric against needle penetration are shown in Figure 7. The measured resistance force increases as the tip of the needle comes in contact with the fabric samples. The maximum force was detected at about 1–2 mm after the tip of the needle penetrates through the coated fabric samples, which matches the sharp-cutting continuous edge of the needle (2 mm). A peak force represents the maximum resistance of textile samples against penetration of hypodermic needles by spreading the fibers away from the tip (windowing mechanism) and cutting the fibers with the sharp conical part (cutting mechanism) [3,30]. The load drops afterward, with minimal resistance against the penetrator. Unlike load-displacement curves shown for the spike test, a second peak was not detected in the needle test. This can be attributed to the lack of resistance of distant fibers near the point of impact due to the small size of the needle compared with the spike penetrator. Maximum resistance force, bending angle, and areal density histogram plots of 1-layer and multiple-layer neat and coated fabric samples are presented in Figure 8.

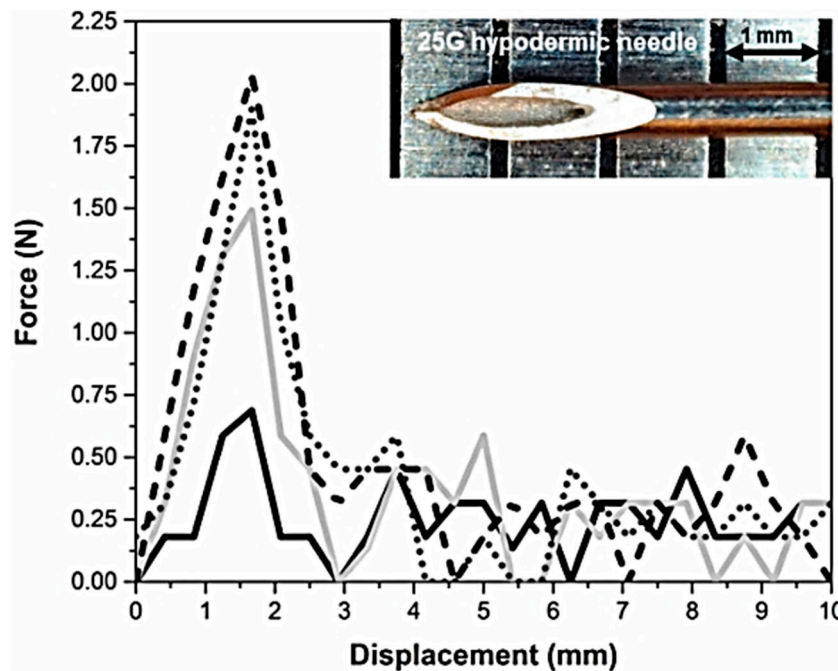


Figure 7. Force-versus-displacement graphs from the 25G needlestick penetration test on single-layer plasma-treated UHMWPE fabric samples: —, neat; - - -, coated with PU; •••, coated with 30 wt.% SiC in PU; - · - ·, coated with 50 wt.% SiC in PU.

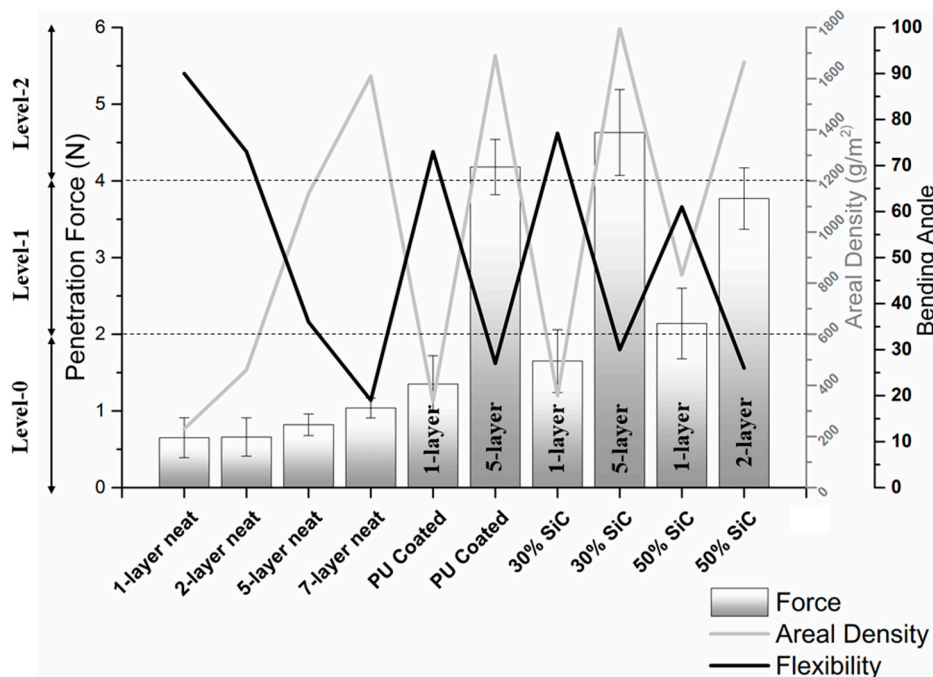


Figure 8. Measured peak resistance force, bending angle, and areal density of plasma-treated neat and coated UHMWPE fabric of various layers undergoing 25G needle penetration tests.

It is observed that the resistance force of 1-layer neat fabric (0.65 ± 0.26 N) does not change significantly compared to 2-layer, 5-layer, and 7-layer neat samples, and even a 7-layer stack of neat fabric is still Level-0 resistance. Coating a 1-layer fabric with 0 wt.%, 30 wt.%, and 50 wt.% SiC in PU mixture increases average penetration resistance by about 108%, 154%, and 229%, respectively.

Furthermore, the normalized penetration resistance force of 1-layer coated fabric with 0 wt.% and 30 wt.% particle was found to be 41% and 62% higher, respectively, than 1-layer neat fabric. Among the coated samples, only 1-layer coated fabric with 50 wt.% SiC is considered as Level-1 protection. However, the normalized force of 1-layer coated fabric with 50 wt.% particle is lower than the neat one (Table S3 in Supplementary Information).

Multiple layers of neat and coated samples were tested to investigate the effectiveness of the coating material based on areal density, flexibility, and thickness. For this purpose, several layers of fabric samples of comparable areal density were stacked together and tested against needlestick penetration. The normalized penetration resistance force of a 7-layer neat fabric ($0.64 \times 10^{-3} \text{ N}/(\text{g}/\text{m}^2)$) increased significantly due to coating, which is about 283, 298, and 251% for 5-layer coated fabric with PU, 5-layer coated fabric with 30 wt.% of SiC, and 2-layer coated fabric with 50 wt.% of SiC, respectively. The highest resistance obtained was at level-2 for the 5-layer coated fabric with PU and also 5-layer coated fabric with 30 wt.% of SiC. These findings show that addition of SiC containing PU coating to UHMWPE does improve needle penetration resistance but only to level-2 (Table S1 in Supplementary Information). In contrast, we have shown previously that particle-laden elastomeric mixtures impregnated into high-count (60×60) HDPE can provide a significant increase in penetration resistance (190%) and produce a level-5 resistance level towards needle penetration threats [3] through an elastic jamming mechanism. The differences in the results may largely be related to the fabric used. The lower thread-count of the UHMWPE (21×21) here results in the lower penetration force for the neat fabric as compared to the HDPE [3]. The higher baseline resistance enabled the HDPE fabric to achieve level-5 performance when the nanoparticle composite was incorporated. Nevertheless, the looser weave of the UHMWPE fabric allows better incorporation of the nanoparticle/PU mixture, and therefore a higher percentage increase in normalized penetration resistance was observed. Such an interpretation is analogous to a similar study that interprets more effective response of innately infirm UHMWPE fabrics to STF-impregnation [15].

4. Conclusions

We showed the considerable impact of coating UHMWPE fabric with a mixture of SiC and polyurethane (PU) to improve spike and hypodermic penetration resistance. A simple dip coating process to incorporate nanoparticle-elastomer mixtures with up to 50 wt.% particle loading was also demonstrated. Spike puncture tests performed on coated fabric show a significantly higher resistance than neat fabric and the resistance increased with increase in SiC content. The penetration resistance of coated fabric was also higher than the neat fabric, even when different stacks of samples of comparable areal density were compared. Further, 5-layer and 2-layer stacks of coated fabric with a mixture of 30 wt.% and 50 wt.% SiC in PU showed up to 57% higher spike-puncture resistance and better flexibility compared to a 7-layer stack of neat fabric of comparable areal density, with 21–55% less thickness. The higher resistance of coated samples can be attributed to a combination of penetration of the coating into the fabric, better adhesion of coating material with the fibers, and the effect of the loaded nanoparticles in exerting more frictional force to the impactor. We also showed that plasma treatment is a crucial preparation process for UHMWPE fabric to improve the adhesion and integration of coating material to the fabric. Non-uniform coatings and poor penetration and puncture resistances were obtained without plasma treatment. Similarly, the resistance of coated fabrics against a 25G hypodermic needle was superior to the neat fabric (up to 298% increase in normalized penetration resistance due to the treatment). The combination of SiC nanoparticles with PU elastomer provides an interesting solution for increasing the puncture resistance while not affecting the needle penetration significantly. In the future, this property could be used on UHMWPE textiles, which have rather weak resistance against puncture threats, in order to improve their robustness and overall performance against a multitude of threats.

Supplementary Materials: The following are available online at <http://www.mdpi.com/2079-6439/7/5/46/s1>, Table S1: Classification for puncture resistance for hand protection against a spike and hypodermic 25G needle

according to the American National Standard Institute/International Safety Equipment Association (ANSI/ISEA 105-2016) standards. Table S2: Absolute and normalized penetration resistance force of plasma-treated neat and coated UHMWPE fabrics against a spike. Table S3: Absolute and normalized penetration resistance force of plasma-treated neat and coated UHMWPE fabrics against a 25 G hypodermic needle. Figure S1: The schematic of fabrication process and plasma treatment setup.

Author Contributions: D.F. was involved in conceiving the idea, performed experiments, analyzed results, wrote the first draft of the paper; P.R.S. and C.Y.C. were involved in conception of the idea, analyzed results, revised the manuscript; S.N.R. contributed to discussions and revised manuscript.

Funding: This research was funded by the Natural Sciences and Engineering Research Council of Canada (NSERC) under the Discovery and Engage programs. It was also supported by the Canada Research Chairs Program.

Conflicts of Interest: The authors declare that there is no conflict of interest regarding the publication of this article.

References

1. Cotter, A. Firearms and Violent Crime in Canada. Statistics Canada. Available online: <https://www150.statcan.gc.ca/n1/pub/85-005-x/2018001/article/54980-eng.htm> (accessed on 28 June 2018).
2. Firouzi, D.; Foucher, D.A.; Bougherara, H. Nylon-Coated Ultra High Molecular Weight Polyethylene Fabric for Enhanced Penetration Resistance. *J. Appl. Polym. Sci.* **2014**, *131*, 40350. [CrossRef]
3. Firouzi, D.; Russel, M.K.; Rizvi, S.N.; Ching, C.Y.; Selvaganapathy, P.R. Development of flexible particle-laden elastomeric textiles with improved penetration resistance to hypodermic needles. *Mater. Des.* **2018**, *156*, 419–428. [CrossRef]
4. Decker, M.K.; Halbach, C.J.; Nam, C.H.; Wagner, N.J.; Wetzel, E.D. Stab resistance of shear thickening fluid (STF)-treated fabrics. *Compos. Sci. Technol.* **2007**, *67*, 565–578. [CrossRef]
5. Cheeseman, B.A.; Bogetti, T.A. Ballistic impact into fabric and compliant composite laminates. *Compos. Struct.* **2003**, *61*, 161–173. [CrossRef]
6. Park, J.; Yoon, B.; Paik, J.; Kang, T. Ballistic performance of *p*-aramid fabrics impregnated with shear thickening fluid; Part I—Effect of laminating sequence. *Text. Res. J.* **2012**, *82*, 527–541. [CrossRef]
7. Park, J.; Yoon, B.; Paik, J.; Kang, T. Ballistic performance of *p*-aramid fabrics impregnated with shear thickening fluid; Part II—Effect of fabric count and shot location. *Text. Res. J.* **2012**, *82*, 542–557. [CrossRef]
8. Sanhita, D.; Jagan, S.; Shaw, A.; Pal, A. Determination of inter-yarn friction and its effect on ballistic response of para-aramid woven fabric under low velocity impact. *Compos. Struct.* **2015**, *120*, 129–140.
9. Lane, R.A. High performance fibers for personnel and vehicle armor systems. *Amptiac Q.* **2005**, *9*, 3–9.
10. Langston, T. An analytical model for the ballistic performance of ultra-high molecular weight polyethylene composites. *Compos. Struct.* **2017**, *179*, 245–257. [CrossRef]
11. Zhang, B.; Nian, X.; Jin, F.; Xia, Z.; Fan, H. Failure analyses of flexible ultra-high molecular weight polyethylene (UHMWPE) fiber reinforced anti-blast wall under explosion. *Compos. Struct.* **2018**, *184*, 759–774. [CrossRef]
12. Kurtz, S.M. Chapter 17—Composite UHMWPE Biomaterials and Fibres. In *UHMWPE Biomaterials Handbook*, 2nd ed.; Academic Press: Burlington, MA, USA, 2009; pp. 249–258.
13. Lin, S.P.; Han, J.L.; Yeh, J.T.; Chang, F.C.; Hsieh, K.H. Surface modification and physical properties of various UHMWPE-fiber-reinforced modified epoxy composites. *J. Appl. Polym. Sci.* **2007**, *104*, 655–665. [CrossRef]
14. Firouzi, D.; Youssef, A.; Amer, M.; Srouji, R.; Amleh, A.; Foucher, D.A.; Bougherara, H. A new technique to improve the mechanical and biological performance of ultra high molecular weight polyethylene using a nylon coating. *J. Mech. Behav. Biomed. Mater.* **2014**, *32*, 108–209. [CrossRef]
15. Arora, S.; Majumdar, A.; Butola, B.S. Structure induced effectiveness of shear thickening fluid for modulating impact resistance of UHMWPE fabric. *Compos. Struct.* **2019**, *210*, 41–48. [CrossRef]
16. Li, W.; Xiong, D.; Zhao, X.; Sun, L.; Liu, J. Dynamic stab resistance of ultra-high molecular weight polyethylene fabric impregnated with shear thickening fluid. *Mater. Des.* **2016**, *102*, 162–167. [CrossRef]
17. Wagner, N.; Wetzel, E.D. Advanced Body Armor Utilizing Shear Thickening Fluids. U.S. Patent 7498276 B2, 3 March 2009.
18. Rao, H.M.; Hosur, M.V.; Jeelani, S. Chapter 12—Stab characterization of STF and thermoplastic-impregnated ballistic fabric composites. In *Advanced Fibrous Composite Materials for Ballistic Protection*; Chen, X., Ed.; Woodhead Publishing: Sawston, UK, 2016; pp. 363–387.

19. Kalman, D.P.; Merrill, R.L.; Wagner, N.J.; Wetzel, E.D. Effect of particle hardness on the penetration behavior of fabrics intercalated with dry particles and concentrated particle-fluid suspensions. *J. Appl. Polym. Sci.* **2009**, *1*, 2602–2612.
20. Asija, N.; Chouhan, H.; Gebremeskel, S.A.; Bhatnagar, N. Impact response of shear thickening fluid (STF) treated high strength polymer composites—Effect of STF intercalation method. *Proc. Eng.* **2017**, *173*, 655–662. [[CrossRef](#)]
21. Asija, N.; Chouhan, H.; Gebremeskel, S.A.; Singh, R.K.; Bhatnagar, N. High strain rate behavior of STF-treated UHMWPE composites. *Int. J. Impact Eng.* **2017**, *110*, 359–364. [[CrossRef](#)]
22. Majumdar, A.; Laha, A.; Bhattacharjee, D.; Biswas, I. Tuning the structure of 3D woven aramid fabrics reinforced with shear thickening fluid for developing soft body armour. *Compos. Struct.* **2017**, *178*, 415–425. [[CrossRef](#)]
23. Joshi, M.; Butola, B.S. Application technologies for coating, lamination and finishing of technical textiles. In *Advances in Dyeing and Finishing of Technical Textiles*; Woodhead Publishing Ltd.: Cambridge, UK, 2013; pp. 355–411.
24. He, R.; Niu, F.; Chang, Q. The effect of plasma treatment on the mechanical behavior of UHMWPE fiber-reinforced thermoplastic HDPE composite. *Surf. Interf. Anal.* **2017**, *50*, 73–77. [[CrossRef](#)]
25. Lehocky, M.; Drnovska, H.; Lapcikova, B.; Barros-Timmons, A.M.; Trindade, T.; Zembala, M.; Lapcik, L., Jr. Plasma surface modification of polyethylene. *Coll. Surf. A Physicochem. Eng. Asp.* **2003**, *222*, 125–131. [[CrossRef](#)]
26. Liu, H.; Xie, D.; Qian, L.; Deng, X.; Leng, Y.X.; Huang, N. The mechanical properties of ultrahigh molecular weight polyethylene (UHMWPE) modified by oxygen plasma. *Surf. Coat. Technol.* **2011**, *205*, 2697–2701. [[CrossRef](#)]
27. Lee, S.G.; Kang, T.J.; Yoon, T.H. Enhanced interfacial adhesion of ultra-high molecular weight polyethylene (UHMWPE) by oxygen plasma treatment. *J. Adhes. Sci. Technol.* **1998**, *12*, 731–748. [[CrossRef](#)]
28. Moon, S.I.; Jang, I. The effect of the oxygen-plasma treatment of UHMWPE fiber on the transverse properties of UHMWPE-fiber/vinylester composites. *Compos. Sci. Technol.* **1999**, *59*, 487–493. [[CrossRef](#)]
29. Roy, R.; Laha, A.; Awasthi, N.; Majumdar, A.; Butola, B.S. Multi layered natural rubber coated woven P-aramid and UHMWPE fabric composites for soft body armor application. *Polym. Compos.* **2017**, *39*, 3636–3644. [[CrossRef](#)]
30. Houghton, J.M.; Schiffman, B.A.; Kalman, D.P.; Wetzel, E.D.; Wagner, N.J. Hypodermic needle puncture of shear thickening fluid (STF)—treated fabrics. In Proceedings of the SAMPE, Baltimore, MD, USA, 3–7 June 2007; pp. 1–11.
31. Kanesalingam, S.; Nayak, R.; Wang, L.; Padhye, R.; Arnold, L. Stab and puncture resistance of silica-coated Kevlar-wool and Kevlar-wool-nylon fabrics in quasistatic conditions. *Text. Res. J.* **2018**, 1–17. [[CrossRef](#)]
32. Sun, L.L.; Xiong, D.S.; Xu, C.Y. Application of shear thickening fluid in ultra high molecular weight polyethylene fabric. *J. Appl. Polym. Sci.* **2013**, *129*, 1922–1928. [[CrossRef](#)]

